

# **CHAPTER V- DESIGN OF A NOVEL POTENTIAL MULTI EPITOPE-BASED SUBUNIT VACCINE TARGETING STRUCTURAL PROTEINS OF DENGUE VIRUS 2**

## 5.1 Introduction

Dengue is a serious global health concern affecting mostly the sub-tropical and tropical regions of the world. It is a mosquito-borne viral infection caused by Dengue virus (DENV) primarily transmitted by female *Aedes aegypti* and *Aedes albopictus* mosquitoes. Non-vector transmission of DENV via blood transfusion, injuries, organ transplantation, and mucosal splashes is also recorded[1]. An estimated 390 million cases of dengue fever are reported each year, with Asia bearing the most of the disease's transmission. The rate of incidence has increased alarmingly due to reasons such as fast urbanization, population development, temperature rise, and insufficient mosquito control measures [2]. The number of dengue cases has gradually increased in India in the last decade as the temperature and climatic conditions in this region support the virus development and transmission[3, 4].

DENV has antigenetically distinct four serotypes DENV1, DENV2, DENV3, and DENV4. However, in October 2013, the fifth variation of DENV-5 was identified. Unlike the other four serotypes, which follow the human cycle, this one follows the sylvatic cycle[5 ].

Though dengue fever is an illness that resembles the flu and can strike both adults and small children, in rare cases, it can be fatal. DENV can cause a variety of clinical symptoms, ranging from mild to severe dengue. Patients with dengue fever experience symptoms such as vomiting, headaches, fever, stomach pain, and maculopapular rash after an incubation period of 4–7 days[7]. Severe bleeding, thrombocytopenia, vascular permeability, plasma leakage, and organ damage are among the signs of severe dengue cases that have been documented[8]. Currently, dengue fever has no known prevention measures or targeted therapeutics; nevertheless, infections can be controlled by identifying cases as soon as possible and initiation of rehydration therapy[9].

The requirement to offer protection against all four dengue serotypes in order to prevent possibly triggering antibody-dependent enhancement in subsequent infections has made the development of dengue vaccines difficult. Dengue vaccines are being developed using several methods, including DNA, recombinant proteins, inactivated viruses, chimeric live attenuated viruses, and live attenuated viruses. These methods are currently undergoing various stages of clinical trials. Licensed dengue vaccines available at this time are

Dengvaxia and Qdenga, however, phase III clinical studies for vaccine TV-003/TV-005 is now being conducted and showing encouraging results[10, 11]. The efficacy and safety of Dengvaxia is in question as studies have reported that the protective efficacy of Dengvaxia depended on prior dengue serostatus of the individuals and has been shown to increase the risk of severe disease in dengue seronegative individuals[12, 13]. In children with < 9 years old and dengue-naïve individuals, lower efficacy of the vaccine was observed. Compared to other serotypes, Dengvaxia is not very efficient against the DENV-2 strain, according to clinical research[14]. This makes the development of a novel vaccine candidate that is effective against the dengue virus strain DENV-2 crucial. In addition to conferring immunity against pathogens, vaccines are thought to be a highly effective means of controlling infectious diseases. Moreover, as drug-based therapy carries the potential for toxicity, vaccines can also be used to prevent it. Many side effects also come along with vaccination, some common symptoms include allergic reactions, headache, fatigue, body aches, fever, abdominal pain, nausea and vomiting, urticaria, and asthma. However an unexpected outcomes of Dengvaxia clinical trials indicated a contraindication for pregnant or lactating women[15], hence more studies are essential to confirm the efficacy of this vaccine. Qdenga is found to be effective in preventing children and adolescents from developing symptoms of dengue. On the other hand, immunocompromised people and pregnant and lactating women should not use it [16-17]. However efficacy for Qdenga is found to be 76.1% in seropositive and 66.2% in seronegative individuals [18]

Using reverse vaccinology, a potential vaccine can be designed in a relatively short period as compared to attenuated and subunit vaccines. This approach is used in developing an epitope-based recombinant vaccine against Malaria termed as RTS,S and successfully reached phase-III trials[19]. Multimeric-001 (M-001) is also another example of an epitope-based Influenza vaccine produced from NP, HA, and M1 proteins conserved epitopes of influenza type A and B strains nine conserved immunogenic epitopes. M-001 has shown to provide protection against multiple influenza strains in animal studies and also human clinical trials have been conducted[20,21].

In this study, we designed a potential novel multi-epitope subunit vaccine using a combination of B cell, T cell, and IFN $\gamma$  epitopes, that would produce strong humoral, cellular, and innate immunity. A multiepitope vaccine construct overcomes the

constraints of a simple peptide vaccine and since these are straightforward peptide sequences, these can be synthesized in a laboratory and thus is a safer option, as it does away with handling of pathogen.

## **5.2 Materials and method**

### **5.2.1 Dengue protein sequence**

Complete sequence of flavivirus polyprotein of DENV type 2 (GenPept: AAA42962) was downloaded from the NCBI protein database. Structural proteins of DENV2 i.e Envelope, PrM and capsid proteins were selected as targets for epitope prediction.

### **5.2.2 B cell linear epitope prediction**

Certain regions of antigens that are recognized by immunological B-cell antibodies are known as B cell epitopes. We have used the BepiPred 2.0 server[22] to predict the linear B-cell epitopes of the DENV structural proteins. Residues that have scores higher than the cutoff point (0.5 by default) are anticipated to form an epitope. B-cell epitopes predicted were served as a template for CTL and HTL epitopes throughout the creation of the final vaccine sequence. T cell epitopes overlapping with B cell epitopes were selected and used in the vaccine's final construction.

### **5.2.3 Cytotoxic T Lymphocytes (CTL) epitope prediction**

Two distinct methods NetCTL 1.2[23] and IEDB NetMHC pan 4.1 EL[24] were used to predict 9-mer peptide length cytotoxic T lymphocytes (CTL) epitopes of DENV2 structural proteins. NetCTL 1.2 is a publicly available web server, where three methods are combined in prediction: TAP transport efficiency, proteasomal C-terminal cleavage, and MHC class-I binding affinity. Twelve MHC class-I super-type restrictions limited the prediction of CTL epitopes in NetCTL 1.2. NetMHC pan 4.1 EL predictions assess a peptide's capacity to bind an MHC molecule. In addition, it also takes into account the possibility that the peptide will be presented and processed normally, increasing the likelihood that it will be identified as a T cell epitope. 27 HLA supertype alleles with maximum population coverage (approximately>97%) were selected to identify and predict MHC I binding epitopes.

### **5.2.4 Helper T Lymphocytes (HTL) epitope prediction**

IEDB server was used in prediction of 15-mer length T helper cell (HTL) epitopes for

all the structural proteins. NetMHCII 4.1 E.L.[24] and IEDB recommended 2.2 Consensus methods [25] were used to predict 15-mer peptide length Helper T lymphocytes (HTL) epitopes of DENV2 structural proteins. All epitopes were predicted for 27 supertype alleles provide more than 99% population coverage.

### **5.2.5 Antigenicity and allergenicity prediction**

VaxiJen v2.0 was used to determine the antigenicity of the predicted epitopes in our vaccine constructions[26]. Antigen prediction in VaxiJen is based on a variety of protein physiochemical characteristics rather than alignment. To identify the most likely protective antigens among extracellular pathogen proteins, a threshold of  $\geq 0.4$  was considered. Allergenicity of the vaccine construct was predicted by Allertope v.2[27]. Based on the physicochemical characteristics of proteins, the allergenic nature was determined.

### **5.2.6 Prediction of various physicochemical properties**

We have used ProtParam server to determine the physicochemical properties of the vaccine construct[28]. ProtParam can calculate different physicochemical qualities based on the pK values of distinct amino acids. The predicted instability index of a protein defines its status: proteins with values less than 40 are categorised as stable, whereas those with values more than 40 are categorised as unstable. The total hydropathy obtained for each of the samples was used to determine the Grand Average of Hydropathy.

### **5.2.7 Cytokine inducing epitope prediction**

IFNepitope server was used to determine the induction capacity of the predicted HTL epitopes[29]. Based on an analysis of a dataset comprising peptides that induce and those that do not, the server ascertains which epitopes are most likely to induce IFN- $\gamma$ . IL4pred and IL10pred servers were used to determine IL-4 and IL-10 inducing HTL epitope respectively. On both servers, the SVM approach was employed, with the default threshold values maintained at 0.2 and  $-0.3$ , respectively.

### **5.2.8 Codon Adaptation**

The generation of eukaryotic proteins in prokaryotic hosts necessitates codon optimization, as not all synonymous codons in a codon family express different proteins at the same rate in E. coli. Therefore, codon optimization was done on E. coli strain K12 in order to raise the levels of protein expression. For codon optimization, the Java Codon

Adaptation Tool or JCat service was utilized[30]. Codon adaptation index (CAI), and GC-content percentage was then examined for the optimized codon sequence for expression parameters. An appropriate CAI value is more than 0.8, while the ideal GC content falls between 30% and 70%.

#### **5.2.9 Secondary structure prediction**

PSIPRED web server was utilised to estimate the secondary structure of the vaccine construct by using the amino acid sequence [31]. PSIPRED is based on two feed-forward neural networks. The first network made the initial prediction, and the second network used the secondary structure that PSIPRED had predicted as input.

#### **5.2.10 Tertiary structure modeling, refinement and validation**

Tertiary structure of the vaccine construct was modelled using Alphafold 2.0[32]. AlphaFold2 is a deep-learning method that integrates empirical knowledge about protein structure. Multiple-sequence alignment, is utilised by the algorithm. Protein models that are predicted are frequently just as accurate as structures found through experimentation. Best model with highest plddt score was selected for further study. The selected model was refined using GalaxyRefine[33]. It creates ten revised models and gives details about each one in relation to the model that the user input, including RMSD, MolProbity, Clash score, Poor rotamers, Rama favoured, and "GALAXY energy." For docking and in silico cloning, the optimised model derived from GalaxyRefine2 was employed. The 3D model's accuracy was validated by a Ramachandran plot using PROCHECK server[34].

#### **5.2.11 Discontinuous B-cell epitope prediction**

Discontinuous or conformational epitopes were predicted using ElliPro[35]. ElliPro uses 3D protein structures to predict B cell epitopes. The default parameters with a minimum score of 0.5 and a maximum distance of 6 Angstrom was taken as the threshold.

#### **5.2.12 Molecular docking of vaccine with immune receptor TLR3**

Molecular docking of vaccine construct with the immunological receptor TLR-3 (PDB ID-2A0Z) was performed using Cluspro v.2.0 docking program with default settings[36]. Cluspro offers cluster scores using pairwise RMSD energy minimisation and rigid docking, sampling billions of conformations. Using PyMOL software, the final vaccine-

TLR3 construct was visualised

.

### **5.2.13 Molecular dynamics simulation of receptor-ligand complex**

To gain insights into the behaviour and structural integrity of complex, molecular dynamics simulations were conducted over a specific timeframe. These simulations were performed using GROMACS 2020.4 and were divided into distinct phases. All-atom simulation techniques were employed for both the receptors and vaccine constructs, utilizing the GROMOS 54A7 force field to define their parameters[37]. Periodic boundary conditions were applied throughout the simulation, and the complex was hydrated using the Simple Point Charge (SPC) water model within a cubic solvation box. In addition, neutralization of the system was achieved by the introduction of counter ions prior to initiating the simulation. Energy minimization was conducted using the steepest descent algorithm, followed by equilibration procedures. During the initial equilibration step, the NVT canonical ensemble was employed, allowing the system to equilibrate under constant number of particles, volume, and temperature conditions for a duration of 2 nanoseconds. Subsequently, the NPT isobaric-isothermal ensemble was utilized in the second equilibration step to achieve pressure equilibrium over a period of 5 nanoseconds[38]. Following the completion of all preceding steps, the final production run was conducted for a duration of 100 ns.

### **5.2.14 In silico immune simulation**

To assess the immune simulation of the vaccine construct, C-ImmSim server was used [39]. C-ImmSim has the potential to evaluate the immunogenic effect of the proposed vaccine in the event of its administration in humans. The simulation parameters were set to their default values, with 100 adjuvant injections and 1000 antigen injections, respectively. The C-ImmSim server's findings align with the outcomes of real immunological reactions. The server C-ImmSim was utilised to predict interleukin and antibody levels as well as the production of B-cells, T cytotoxic cells, T helper cells, and natural killer cells.

### **5.2.15 Population Coverage analysis**

For immunization to be successful, a vaccine component must offer broad-spectrum protection against diseases in diverse worldwide populations. Consequently, the IEDB

population coverage[40] utility was used to conduct the epitope population coverage analysis. The chosen combined MHC-I and MHC-II peptide data were provided, and the selection process took into consideration all global area.

## **5.3 Results**

### **5.3.1 Viral protein selection for vaccine preparation**

The amino acid sequence of Dengue virus 2 structural proteins i.e Envelope, capsid and prM proteins were retrieved from National Center for Biotechnology Information database GenBank Id(AAA42962.1).

### **5.3.2 Prediction of B-cell epitope.**

B cell linear epitopes of the structural proteins were predicted using IEDB based tool BepiPred 2.0. A total of 27 B Cell linear epitopes were predicted but depending on the overlapping sequence with T cell epitopes only 16 were chosen for further study. B-cell epitopes predicted served as a template for CTL and HTL epitopes throughout the creation of the final vaccine sequence. T cell epitopes whose sequences in B cell epitopes overlapped were selected and used in the vaccine's final construction (Table 5.1).

### **5.3.3 HLA-supertype alleles for T cell epitope prediction**

The primary Human Leukocyte Antigen class I (HLA-I) supertypes, which include African Americans, Caucasians, Hispanics, Asians, and Native Americans, are reported to have more than 97% population coverage over 27 alleles. Similarly, it has been demonstrated that 27 alleles of HLA-II offer more than 99% population coverage.

#### **5.3.3.1 Prediction of T cell epitopes**

Cytotoxic T lymphocytes (CTLs) epitopes were predicted using two different tools which are IEDB NetMHC E.L 4.1 and NetCTL 1.2. Epitopes that fall below the VaxiJen server's 0.4 cutoff level were eliminated and also allergenic epitopes were eliminated and none of the epitopes were found to be toxic. A total of 20, 19 and 43 CTL epitopes of capsid, prM and Envelope proteins respectively were predicted by both tools combined. CTL epitopes predicted by both prediction tools and those overlapping with B- cell epitopes were selected for final vaccine construct (Table 5.1). 12 CTL epitopes were selected



which consisted of 2 capsid, 3 prM and 7 Envelope CTL epitopes.

Helper T cells epitopes were predicted using the IEDB server. Two different prediction methods were used NetMHCII 4.1 E.L and IEDB recommended 2.2(Consensus method). Epitopes that were predicted allergenic and non-antigenic were removed. None of the epitopes were found to be toxic. A total of 6, 12 and 28 HTL epitopes of capsid, prM and Envelope proteins respectively were predicted by both the tools combined. HTL epitopes predicted by both prediction tools and those overlapping with B- cell epitopes were selected for final vaccine construct(Table 5.1). 7 HTL epitopes were choosen for the final vaccine construct which consisted of 1 capsid, 1 prM and 5 Envelope CTL epitopes.

Sl.no	Protein	Sequence	CTL	HTL
1	Capsid	QRKKARNTPFNMLKR ERNRVSTVQQLTKR	RNTPFNMLK	
2		IPPTAGILKRWGTIKK SKAI		WGTIKKSKAINVLRG
3		LNRRRRTA	LNRRRRTAG	
4	prM	RQEKGKSLLFKTEDG	QEKGKSLLF	
5		TTTGEHRREKRSVAL VPHVGMGLETRTETW MSSEGAWKH	REKRSVALV	
6		TTHF	YTIGTTHFQ	THFQRALIFILLTAV
7	Envelope	TEAKQPAT	TEAKQPATL	
8		QSSITEA	ITEAELTGY	
9		GLD	GLDFNEMVL	GLDFNEMVLLQMEDK
10		FLDLPLPWLPGADTQG SNWIQKE		WIKETLVTFKNPHA
11		NPHAK		
12		EIQMS		GATEIQMSSGNLLFT
13		TGKFKVVKEIAETQH	EIAETQHGT	QLKGMSYSMCTGKFK
14		FEIMDLEKRH	MDLEKRHVL	
15		QLKLDWFKKGSS	QLKLDWFKK	
16		WDFGSLGG	SLGGVFTSI	AILGDTAWDFGSLGG

**Table 5.1.** CTL and HTL epitopes selected for vaccine construct. T-cell epitopes selected are shown to be overlapping with B-cell epitopes.

### 5.3.4 Multi-epitope vaccine sequence construction

The linkers AAY and GPGPG respectively, were used to merge a total of 12 CTL and 7 HTL epitopes. EAAAK linker, a 45-amino acid long adjuvant beta-defensin (GIINTLQKYICRVRGGRCVLSCLPKEEQIGKCSTRGRKCCRRKK) was attached to the construct's N-terminal. The length of the final vaccine construct designed was found

to be 331 amino acids long after the addition of linkers and adjuvant. A schematic representation of the vaccine construct is shown below in Figure 5.1.

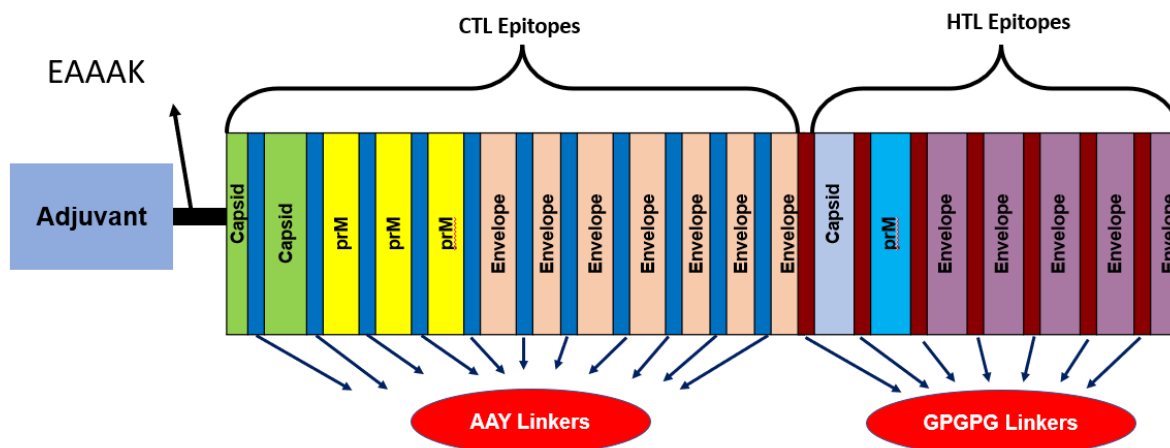


**Figure 5.1-** A Schematic diagram of the vaccine construct. CTL epitopes were joined by AAY linkers (blue) while HTL epitopes were joined by GPGPG linkers (brown). Adjuvant (purple) linked to the epitopes at N-terminal with the help of EAAAK linker (black).

### 5.3.5 Cytokine-inducing capacity prediction of the epitopes

Cytokine-inducing (IL-10, IL-4 and IFN- $\gamma$ ) capacity of all the potential HTL epitopes was checked. Among the seven potential HTL epitopes incorporated in the vaccine construct, 3 epitopes were IL-10 inducing, 6 epitopes were IL-4 inducing and 2 epitopes were IFN- $\gamma$  inducing. Here prM HTL epitope WGTIKKSKAINVLRG was found to be a potent inducer of all three IL-10, IL-4 and IFN- $\gamma$  cytokines.

### 5.3.6 Allergenicity and antigenicity of the vaccine construct.

VaxiJen 2.0 and AllerTOP v. 2 were used to check for antigenicity and allergenicity prediction. The antigenic score of the vaccine construct was 0.7371 which reveals a good antigenic nature of the vaccine construct. And also the vaccine construct was found to be non-allergenic.

### 5.3.7 Physicochemical analysis of vaccine construct.

Physicochemical properties of the vaccine were assessed using the ProtParam server. Physicochemical analysis of the final vaccine construct reveals an instability index score

of 31.03 which indicates the construct is stable. (shown in Table 5.2) The vaccine design appears to be somewhat basic based on the analysis's 9.67 pI (isoelectric point) value and has an estimated half-life of more than ten hours in *Escherichia coli*. The protein is thermostable, as indicated by the estimated aliphatic index of 73.26; a higher aliphatic index value corresponds to greater thermostability. The computed grand average of hydropathicity (GRAVY) was -0.228; a negative number suggests that the protein is hydrophilic and will interact with molecules of water. Overall, the physicochemical characteristics of the vaccine construct were found to be biologically significant, according to ProtParam analysis.

Parameters	Properties
Molecular mass	<b>35.54 k Da</b>
Theoretical P.I	<b>9.67</b>
Half life	<b>&gt;10 hours in E.coli</b>
Instability index	<b>31.03</b>
Aliphatic index	<b>73.26</b>
Grand Average of hydropathicity	<b>-0.228</b>

**Table-5.2-** Physicochemical analysis of vaccine construct

### **5.3.8 Secondary structure prediction.**

The PSIPRED server provided a prediction for the final vaccine construct's secondary structure. It makes secondary structure predictions based on the protein's amino acid sequence. A construct spanning 331 amino acids was examined, of which 146 amino acids were implicated in the creation of coils and 106 amino acids were involved in the construction of the  $\alpha$ -helix, whereas just 79 amino acids are needed to make the  $\beta$ -strands. Overall, the secondary structure prediction result shows that 23.86% of the structure is stranded, 32.12% is helix, and 44.12% is coil (Figure-5.2).

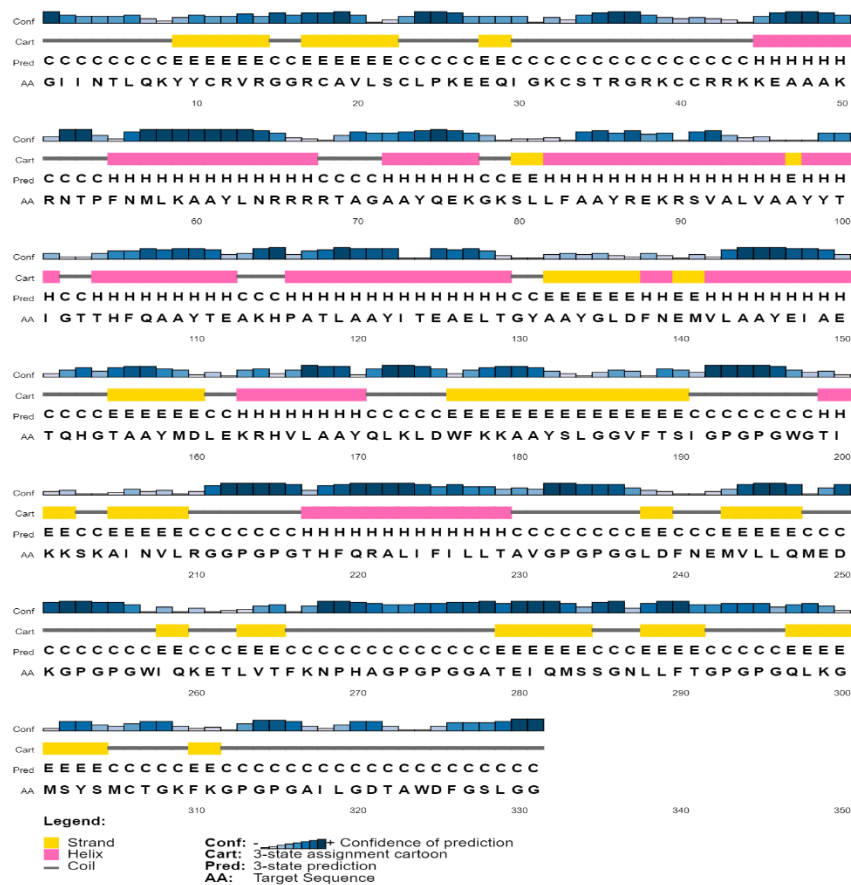


**Figure 5. 2-.** A representation of secondary structure of the vaccine construct consisting of alpha-helix (32.12%),  $\beta$ -strands (23.86%) and coils (44.12%).

### 5.3.9 Tertiary structure modelling

3D model of the vaccine construct was modelled using AlphaFold 2 (Figure 5.3a). Subsequently, the vaccine's modelled structure was improved by Galaxy Refine and verified with the Ramachandran. PyMOL was used to overlay the 3D structures of the initial model and the best refined model in order to display conformational changes that occurred during refinement (Figure 5.3b). The vaccine protein's amino acid composition was shown by the Ramachandran plot to contain 97.4% of the amino acids in the most favoured region, 2.2% in allowed regions, and 0.4% in the generously allowed region Figure-5.3c.

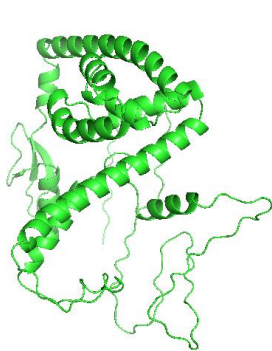


**Figure- 5.3a** 3D Model of vaccine construct

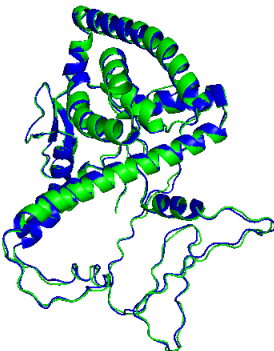


**Figure 5.3b**-Comparison of tertiary protein structures. The initial and the refined model are colored in green and blue, respectively

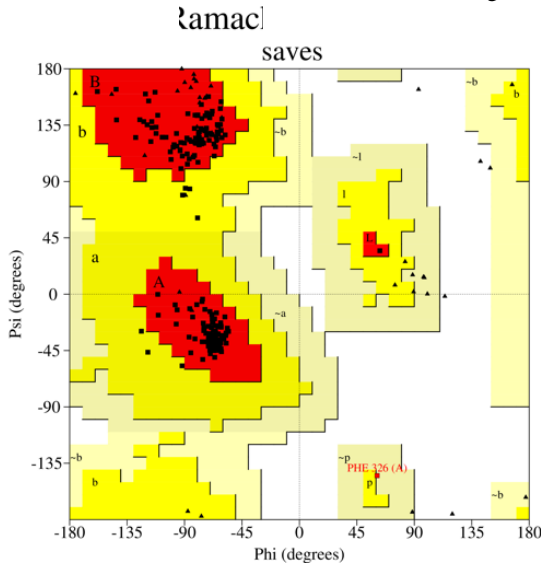


**Figure 5.3c**- Validation of multi-epitope vaccine tertiary structure by Ramachandran plot where 97.4% residues were found in the favored region, 2.2% residues were found in allowed region and 0.4% residues were lies in generously allowed region.

**5.3.10 Prediction of discontinuous B-cell epitope.**

Predicted discontinuous B cell epitopes are represented in Table 5.3. 16 conformational B cell epitopes were predicted to be present on the vaccine construct.

No	Residues	No of residues	Score
1	A:G327, A:S328, A:L329, A:G330, A:G331	5	0.955
3	A:N268, A:P269, A:H270, A:A271, A:G272, A:P273, A:G274, A:P275, A:G276, A:G277, A:A278, A:T279, A:E280, A:I281, A:Q282	15	0.799
4	A:F290, A:T291, A:G292, A:P293, A:G294, A:P295, A:G296, A:Q297, A:L298	9	0.794

5	A:K309, A:F310, A:K311, A:G312, A:P313, A:G314, A:P315, A:G316, A:A317, A:I318, A:L319, A:G320, A:D321, A:T322, A:A323, A:W324, A:D325, A:F326	18	0.788
6	A:E46, A:A49, A:K50, A:N52, A:T53, A:P54, A:F55, A:N56, A:M57, A:L58, A:K59	11	0.76
7	A:D250, A:K251, A:G252, A:P253, A:G254, A:P255, A:G256, A:W257, A:I258, A:Q259, A:K260	11	0.734
8	A:Q107, A:A108, A:A109, A:Y110, A:T111, A:E112, A:A113, A:K114, A:H115, A:T118	10	0.72
9	A:G1, A:I3, A:N4, A:G16, A:R17, A:C18, A:A19, A:V20, A:L21, A:S22, A:C23, A:L24, A:P25, A:K26, A:E27, A:Q29, A:K32, A:C33, A:S34, A:T35, A:R36, A:G37, A:R38, A:K39, A:C41, A:R43	26	0.712
10	A:A60, A:A61, A:Y62, A:R65, A:R66	5	0.679
11	A:T69, A:A72, A:A73, A:E76, A:K77	5	0.647
12	A:G211, A:G212, A:P213, A:G214, A:P215, A:G216, A:T217	7	0.634
13	A:K79, A:S80, A:L81, A:A84, A:R87, A:E88, A:R90	7	0.623
14	A:G102, A:T103, A:T104, A:H105	4	0.547
15	A:E261, A:T262, A:L263, A:V264, A:T265	5	0.517
16	A:K202, A:S203, A:K204, A:A205, A:N207, A:R210	6	0.505

**Table 5.3-** Discontinuous B-cell epitopes of the vaccine construct

### 5.3.11 Molecular docking of final vaccine construct with immunological receptor TLR3

Using online server ClusPro v.2.0, molecular docking was carried out to assess the interaction between the refined vaccine model and the immunological receptor TLR-3 (PDB ID-2A0Z). When all 10 docked conformations were analysed, the best docked model from the ClusPro v.2.0 docking output was chosen for further examination. Because it depicts the important interactions His539 and Asn541 between the receptor and the ligand, model number 7 was the best-docked model.

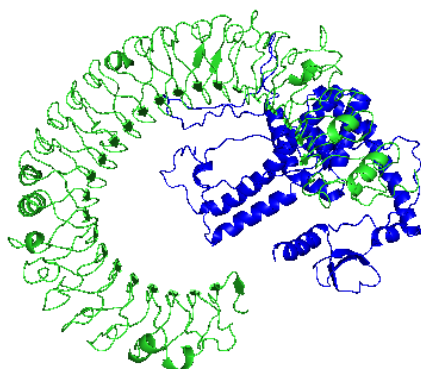


**Figure -5.4a-** Vaccine-TLR3 docked complex

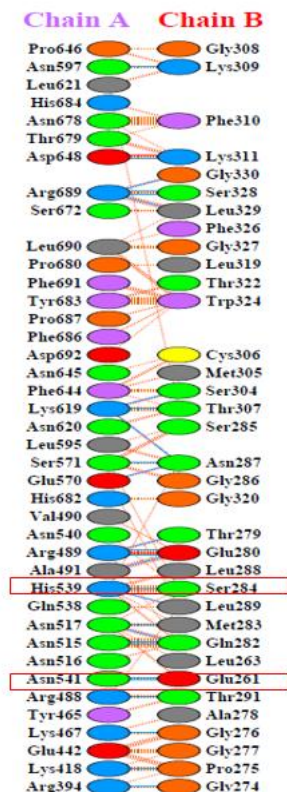


**Figure 5.4b-** Interacting residues between Vaccine and TLR3

### 5.3.12 Molecular Dynamics simulation

The Root Mean Square Deviation (RMSD) analysis of the TLR3 protein indicated stability within the range of 0.5 to 0.75 nanometers, while the vaccine construct exhibited fluctuations ranging from 1 to 1.75 nanometers in Figure.5.5a. Both entities demonstrated comparable stability over the simulation period. Root Mean Square Fluctuation (RMSF) analysis in Figure 5.5-b revealed fluctuations in specific regions, with TLR3 displaying fluctuations between amino acids 600 and 700, and the vaccine construct between amino acids 180 and 210. Radius of gyration (Rg) analysis demonstrated substantial compactness for both TLR3 and the construct in Figure 5.5-c. Moreover, hydrogen bond analysis in Figure 5.5-d indicated a range of 20 to 30 bonds in the initial simulation phase, increasing to 30 to 35 bonds later on. Overall, the TLR3-construct complex exhibited stability and compactness based on the analysis results.

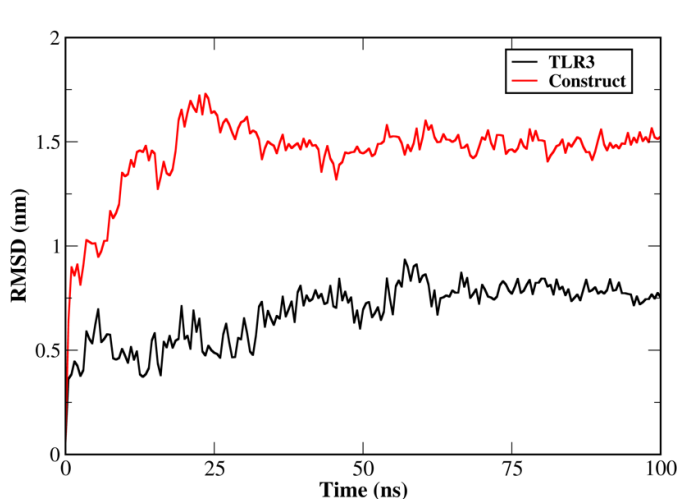


**Figure 5.5 a:** RMSD of TLR3 and vaccine construct.

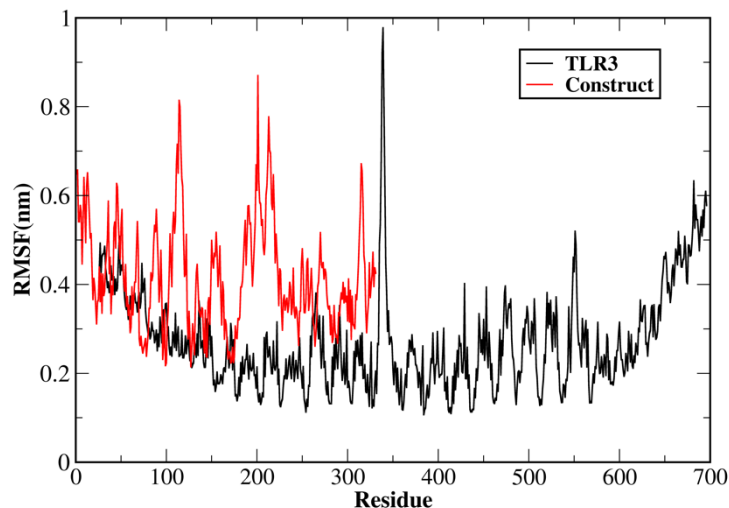


**Figure 5.5 b:** RMSF of TLR3 and vaccine construct.

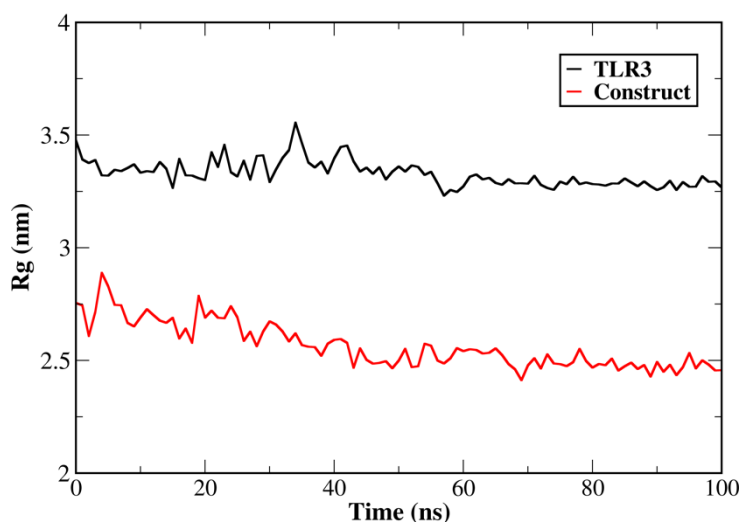


**Figure 5.5 c:** Rg of TLR3 and vaccine construct.

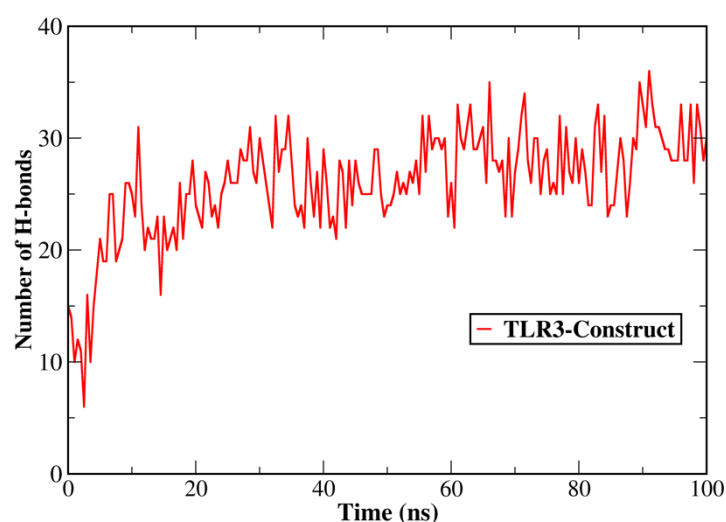


**Figure 5.5 d:** H-bond plot of TLR3-vaccine complex.

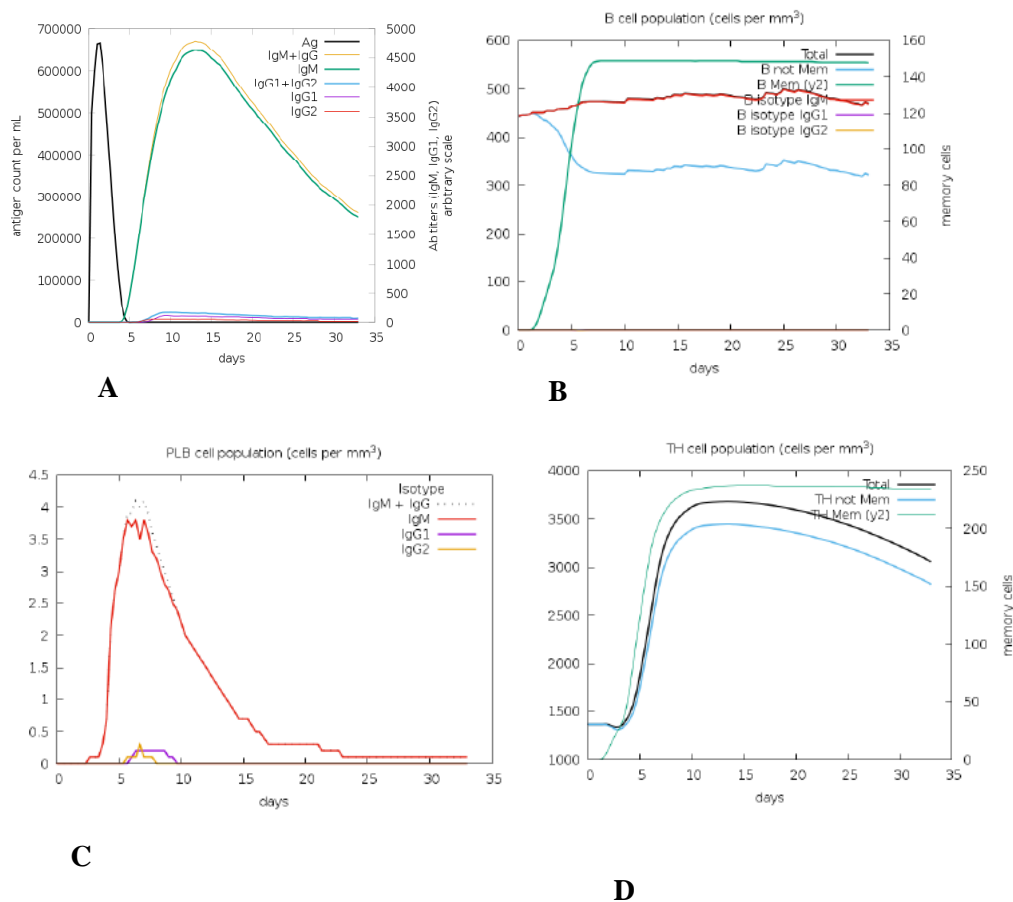
### 5.3.13 Codon Adaptation

The cDNA sequence produced by reverse translation was examined using codon optimization analysis. Codon optimization assesses the sequence and provides information about the GC content of the cDNA sequence as well as the codon adaptive index (CAI). The GC content was determined to be 53.37%, falling within the optimal range of 30–70%, and the CAI was determined to be 1.00, falling within the same range (0.8–1.0). A high value of the CAI indicates high gene expression.



### 5.3.14 In silico immune simulation

Immune simulation study showed a consistent increase in the levels of various immunoglobulins, such as IgG1 + IgG2 and IgG + IgM antibodies (Figure 5.6A), which might significantly boost the initial immune response to the vaccine following vaccination. Additionally, a steady increase in the concentrations of cytotoxic T cells, helper T cells, plasma B cells, and active B cells was predicted, indicating the vaccine's ability to produce a strong secondary immunological response and a robust immune memory. Increased level of dendritic cell and macrophage cells concentrations showed that these APCs had a competent presentation of antigen. According to the simulation outcome, the developed vaccine may also produce a variety of cytokines, including as IFN- $\gamma$ , TGF- $\beta$ , IL-10, and IL-2, which are among the most important cytokines for eliciting an immune response against viral infections . Consequently, the overall immunological simulation analysis demonstrated that the suggested multi-epitope vaccine would be capable of eliciting a strong immune response following administration.



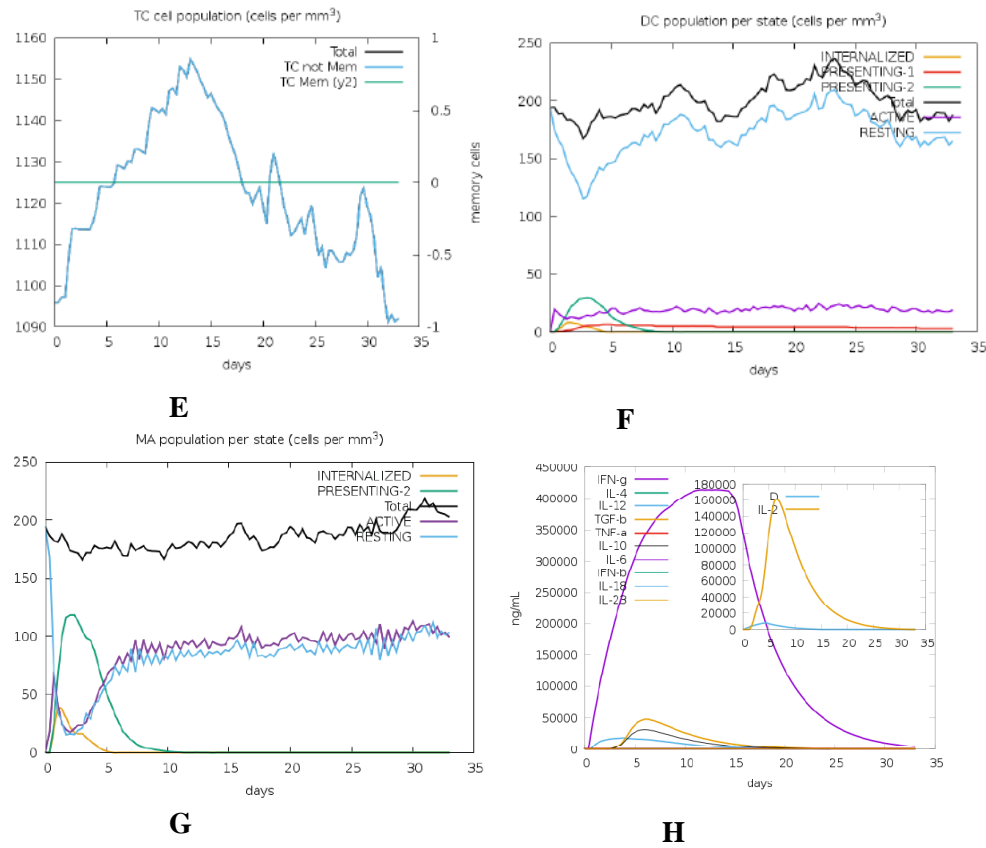


**Figure 5.6.** Representation of the immune simulation performed using C-IMMSIMM. (A) Immunoglobulin response to the vaccine injection (black line) and specific subclasses of immunoglobulins are indicated by coloured lines, (B,) B-cell population, (C) Rise in the plasma B-cell population, (D) Increase of the helper T-cell population, , (E) Increase in the cytotoxic T lymphocyte population throughout the injections, (F,G,) Dendritic cell and macrophage cell stimulus, (H) Level of different types of cytokines induced by injection.

### 5.3.15 Population coverage of selected epitopes

Population coverage analysis showed that the selected epitopes cover 95–100% of the world's population. The figure 5.7 shows the population coverage percentage of various regions of the world.

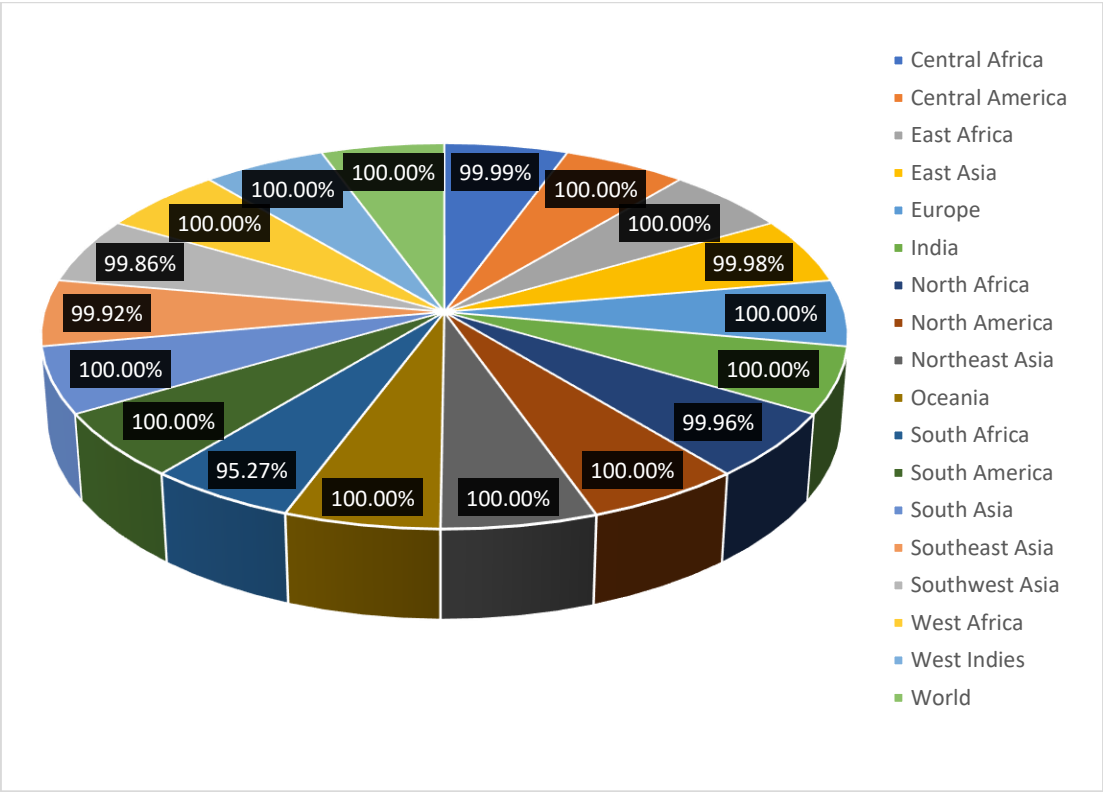


**Figure 5.7-** Population coverage map of selected CTL and HTL epitopes.

#### 5.4 Discussion

Effective treatment must be developed to control the rising incidence of Dengue, especially in places where the Aedes mosquitoes are endemic. To date, efforts to develop a vaccine that could prevent Dengue or an effective medication to treat it have not proven successful. Due to the health hazards involved, the use of "DENG VAXIA," the first dengue vaccine, has been deemed controversial and has various limitations[41,42].

The capacity of a prospective vaccine candidate to elicit strong immune responses is a crucial feature. The goal of the vaccination is to imitate the presence of the target pathogen—a virus, for example—without actually causing the illness. A vaccine formulation contains antigens or parts of the pathogen that trigger the immune system. Invasion of the host cell is one of the early processes in establishing an infection and is mediated by viral structural proteins and this makes these molecules an attractive target of host immune response.

The advantage of reverse vaccinology is that it can speed up the otherwise drawn-out and laborious vaccine development process. Due to its great specificity, stability, safety, and cost-effectiveness, this has been used in the development of multiepitope subunit vaccines

against multiple infectious pathogens. Multi-epitope vaccines against a variety of infections, such as malaria, influenza, and HIV-1, have been developed using this methodology and are currently at different stages of clinical trials.[19]. RTS, S/AS01 is a recombinant epitope-based WHO-recommended malaria vaccine. Phase 3 trials study demonstrated the efficacy of the vaccine against clinical malaria, and severe malaria with a tolerable safety profile in children aged 6 weeks to 17 months[43]. Multimeric-001 (M-001) has also proved to be a good vaccine candidate for influenza in human trials. In young adults between the ages of 18 and 49, the M-001 vaccine produced strong humoral and cell-mediated responses [20] but in the case of elderly people, favorable immunological responses were shown after three weeks of vaccination[44]. These successful clinical reports prove the advancement and efficacy of epitope-based vaccines. B- and T-cell epitopes are necessary for an ideal multi-epitope vaccine to activate a broad immune response. Therefore, CTL, HTL, and B-cell epitopes of DENV structural proteins were used to design a multi-epitope based subunit vaccine. The vaccine construct consisted of 12 antigenic CTL and 7 HTL epitopes linked by AAY and GP GPG, respectively. GP GPG motifs enhance proteasome processing and increase immunogenicity by inducing HTL responses. In mammalian cells, the proteasome cleavage site is AAY. As a result, the AAY linker-linked epitopes are effectively segregated within cells. Additionally, the multi-epitope vaccine's immunogenicity is enhanced by the AAY linker[45,46]. Designing a vaccine that works requires a strong adjuvant that boosts immune responses. Here we have used human  $\beta$ -defensin 3 as an adjuvant because of its antibacterial and immunomodulatory qualities[47]. The presence of conformational B-cell epitopes of the vaccine construct is anticipated to enhance B-cell activation.

DENV structural proteins have their roles and functions. prM protein functions as a molecular chaperone, inhibiting the early fusion of the E protein with host cell membranes. It is cleaved at position 91 by protease which results in pr and M proteins[48]. CTL epitope **REKRSVALV** falls within the cleavage site of prM. CTL epitope **RNTPFNMLK** of capsid lies in the N-terminal (1-22) region which contributes to RNA binding and viral particle formation. Domain II of DENV Envelope protein is crucial for the dimerization of the E protein and harbors the hydrophobic fusion loop that facilitates host cell invasion. In the vaccine construct HTL epitopes **WIQKETLVTFKNPHA** and

**GATEIQMSSGNLLFT** lie in domain ii of Envelope protein. It is anticipated that these epitopes will play a significant role in host defense, making it a possible target for diagnostics and treatments. Domain iii region of DENV envelope protein is the receptor-binding domain and target of potent virus-neutralizing antibodies. Our designed vaccine construct consists of three CTL epitopes **EIAETQHGT**, **MDLEKRHVL**, and **QLKLDWFKK** and one HTL epitope **QLKGMSYSMCTGKFK** which lies in this region, thereby indicating a potential to evoke a specific immune response[49].

Strong immunological responses are elicited by the developed vaccine construct. Molecular docking and molecular dynamics simulations validated the binding affinity and stability of the vaccine construct with immune receptor TLR3. This would result in an efficient downstream signaling cascade and enable innate immunity to develop and effectively combat the pathogen.

Another important factor in designing vaccines is consideration of population coverage. The cumulative percentage of population coverage was measured for all the epitopes incorporated in the vaccine design. The overall population coverage data reveals 95-100% coverage for various regions of the world. This conclusion implied that the vaccine would be effective for the vast majority of people around the world.

## 5.5 References

1. Wilder-Smith, A., et al., *Dengue*. The Lancet, 2019. **393**(10169): p. 350-363.
2. World Health Organisation. *Dengue and severe dengue*. [English] 2023 17 March 2023 [cited 2024 3 April]; Available from: <https://www.who.int>.
3. Mutheneni, S.R., et al., *Dengue burden in India: recent trends and importance of climatic parameters*. Emerging microbes & infections, 2017. **6**(1): p. 1-10.
4. Ganeshkumar, P., et al., *Dengue infection in India: A systematic review and meta-analysis*. PLoS neglected tropical diseases, 2018. **12**(7): p. e0006618.
5. Mustafa, M., et al., *Discovery of fifth serotype of dengue virus (DENV-5): A new public health dilemma in dengue control*. Medical journal armed forces India, 2015. **71**(1): p. 67-70.
6. Dwivedi, V.D., et al., *Genomics, proteomics and evolution of dengue virus*. Briefings in functional genomics, 2017. **16**(4): p. 217-227.
7. Estofolete, C.F., et al., *Unusual clinical manifestations of dengue disease—Real or imagined?* Acta tropica, 2019. **199**: p. 105134.
8. Htun, T.P., Z. Xiong, and J. Pang, *Clinical signs and symptoms associated with WHO severe dengue classification: a systematic review and meta-analysis*. Emerging Microbes & Infections, 2021. **10**(1): p. 1116-1128.
9. Chawla, P., A. Yadav, and V. Chawla, *Clinical implications and treatment of dengue*. Asian Pacific journal of tropical medicine, 2014. **7**(3): p. 169-178.
10. Guy, B., M. Saville, and J. Lang, *Development of Sanofi Pasteur tetravalent dengue vaccine*. Human vaccines, 2010. **6**(9): p. 696-705.
11. Thomas, S.J. and I.-K. Yoon, *A review of Dengvaxia®: development to deployment*. Human vaccines & immunotherapeutics, 2019. **15**(10): p. 2295-2314.
12. Salje, H., et al., *Evaluation of the extended efficacy of the Dengvaxia vaccine against symptomatic and subclinical dengue infection*. Nature medicine, 2021. **27**(8): p. 1395-1400.
13. Thomas, S.J., *Is new dengue vaccine efficacy data a relief or cause for concern?* npj Vaccines, 2023. **8**(1): p. 55.
14. Prompetchara, E., et al., *Dengue vaccine: Global development update*. Asian Pac J Allergy Immunol, 2020. **38**(3): p. 178-185.

15. Kariyawasam, R., et al., *A dengue vaccine whirlwind update*. Therapeutic Advances in Infectious Disease, 2023. **10**: p. 20499361231167274.
16. Lee MF, Ming LC, Poh CL. *Current status of the development of dengue vaccines*. Vaccine: X. 2024 Dec 17:100604.
17. Afzal MF. *Systematic review of Dengue Vaccines (CYD-TDV and TAK-003) in children: efficacy, immunogenicity, safety and challenges*. Journal of Child Health Sciences. 2024 Sep 26.
18. Agustina A, Alamanda CN. *Assessing the Efficacy of Dengue Vaccine: A Comprehensive Literature Review*. Indonesian Journal of Clinical Pathology and Medical Laboratory. 2025 Feb 20;31(2):196-200
19. Oyarzún, P. and B. Kobe, *Recombinant and epitope-based vaccines on the road to the market and implications for vaccine design and production*. Human vaccines & immunotherapeutics, 2016. **12**(3): p. 763-767.
20. Atsmon, J., et al., *Safety and immunogenicity of multimeric-001—a novel universal influenza vaccine*. Journal of clinical immunology, 2012. **32**: p. 595-603.
21. Romeli, S., S.S. Hassan, and W.B. Yap, *Multi-epitope peptide-based and vaccinia-based universal influenza vaccine candidates subjected to clinical trials*. The Malaysian journal of medical sciences: MJMS, 2020. **27**(2): p. 10.
22. Jespersen, M.C., et al., *BepiPred-2.0: improving sequence-based B-cell epitope prediction using conformational epitopes*. Nucleic acids research, 2017. **45**(W1): p. W24-W29.
23. Larsen, M.V., et al., *Large-scale validation of methods for cytotoxic T-lymphocyte epitope prediction*. BMC bioinformatics, 2007. **8**: p. 1-12.
24. Reynisson, B., et al., *NetMHCpan-4.1 and NetMHCIIpan-4.0: improved predictions of MHC antigen presentation by concurrent motif deconvolution and integration of MS MHC eluted ligand data*. Nucleic acids research, 2020. **48**(W1): p. W449-W454.
25. Wang, P., et al., *Peptide binding predictions for HLA DR, DP and DQ molecules*. BMC bioinformatics, 2010. **11**: p. 1-12.

26. Doytchinova, I.A. and D.R. Flower, *VaxiJen: a server for prediction of protective antigens, tumour antigens and subunit vaccines*. BMC bioinformatics, 2007. **8**: p. 1-7.
27. Dimitrov, I., et al., *AllerTOP v. 2—a server for in silico prediction of allergens*. Journal of molecular modeling, 2014. **20**: p. 1-6.
28. Garg, V.K., et al., *MFPPI—multi FASTA ProtParam interface*. Bioinformation, 2016. **12**(2): p. 74.
29. Dhanda, S.K., P. Vir, and G.P. Raghava, *Designing of interferon-gamma inducing MHC class-II binders*. Biology direct, 2013. **8**: p. 1-15.
30. Grote, A., et al., *JCat: a novel tool to adapt codon usage of a target gene to its potential expression host*. Nucleic acids research, 2005. **33**(suppl\_2): p. W526-W531.
31. Buchan, D.W. and D.T. Jones, *The PSIPRED protein analysis workbench: 20 years on*. Nucleic acids research, 2019. **47**(W1): p. W402-W407.
32. Skolnick, J., et al., *AlphaFold 2: why it works and its implications for understanding the relationships of protein sequence, structure, and function*. Journal of chemical information and modeling, 2021. **61**(10): p. 4827-4831.
33. Heo, L., H. Park, and C. Seok, *GalaxyRefine: Protein structure refinement driven by side-chain repacking*. Nucleic acids research, 2013. **41**(W1): p. W384-W388.
34. Laskowski, R.A., et al., *PROCHECK: a program to check the stereochemical quality of protein structures*. Journal of applied crystallography, 1993. **26**(2): p. 283-291.
35. Ponomarenko, J., et al., *Ellipro: a new structure-based tool for the prediction of antibody epitopes*. BMC bioinformatics, 2008. **9**: p. 1-8.
36. Kozakov, D., et al., *The ClusPro web server for protein–protein docking*. Nature protocols, 2017. **12**(2): p. 255-278.
37. Saha, D., N.J. Borah, and A.N. Jha, *Molecular scaffold recognition of drug molecules against essential genes of Leishmania donovani using biocomputing approach*. South African Journal of Botany, 2023. **162**: p. 52-63.
38. Quraishi, S., et al., *Non-covalent binding interaction of bioactive coumarin esculetin with calf thymus DNA and yeast transfer RNA: A detailed investigation to decipher the binding affinities, binding location, interacting forces and*



- structural alterations at a molecular level*. International Journal of Biological Macromolecules, 2024. **257**: p. 128568.
39. Rapin, N., et al., *Computational immunology meets bioinformatics: the use of prediction tools for molecular binding in the simulation of the immune system*. PloS one, 2010. **5**(4): p. e9862.
40. Bui, H.-H., et al., *Predicting population coverage of T-cell epitope-based diagnostics and vaccines*. BMC bioinformatics, 2006. **7**: p. 1-5.
41. Wilder-Smith, A., *Dengue vaccine development by the year 2020: challenges and prospects*. Current opinion in virology, 2020. **43**: p. 71-78.
42. Pintado Silva, J. and A. Fernandez-Sesma, *Challenges on the development of a dengue vaccine: a comprehensive review of the state of the art*. Journal of General Virology, 2023. **104**(3): p. 001831.
43. Syed, Y.Y., *RTS, S/AS01 malaria vaccine (Mosquirix®): a profile of its use*. Drugs & Therapy Perspectives, 2022. **38**(9): p. 373-381.
44. Lowell, G.H., et al., *Back to the future: Immunization with M-001 prior to trivalent influenza vaccine in 2011/12 enhanced protective immune responses against 2014/15 epidemic strain*. Vaccine, 2017. **35**(5): p. 713-715.
45. Chao, P., et al., *Proteomics-based vaccine targets annotation and design of multi-epitope vaccine against antibiotic-resistant Streptococcus gallolyticus*. Scientific Reports, 2024. **14**(1): p. 4836.
46. Davoodi, S., et al., *Design and in vitro delivery of HIV-1 multi-epitope DNA and peptide constructs using novel cell-penetrating peptides*. Biotechnology letters, 2019. **41**: p. 1283-1298.
47. Tahir ul Qamar, M., et al., *Multiepitope-based subunit vaccine design and evaluation against respiratory syncytial virus using reverse vaccinology approach*. Vaccines, 2020. **8**(2): p. 288.
48. Zhang, Q., et al., *The stem region of premembrane protein plays an important role in the virus surface protein rearrangement during dengue maturation*. Journal of Biological Chemistry, 2012. **287**(48): p. 40525-40534.
49. Guzman, M.G., et al., *Domain III of the envelope protein as a dengue vaccine target*. Expert review of vaccines, 2010. **9**(2): p. 137-147.